Atmos. Chem. Phys. Discuss., 14, 13109–13131, 2014
www.atmos-chem-phys-discuss.net/14/13109/2014/
doi:10.5194/acpd-14-13109-2014

Atmospheric Chemistry and Physics
Discussions
Open Access

The decreasing albedo of Zhadang glacier on western Nyainqentanglha and the role of light-absorbing impurities

B. Qu[4,1], J. Ming[1,2,3], S.-C. Kang[1,4], G.-S. Zhang[4], Y.-W. Li[4], C.-D. Li[4], S.-Y. Zhao[5], Z.-M. Ji[4], and J.-J. Cao[5]

[1]State Key Laboratory of Cryospheric Sciences, Cold and Arid Regions Environmental and Engineering Research Institute, Chinese Academy of Sciences,Lanzhou, China
[2]Collaborative Innovation Center on Forecast and Evaluation of Meteorological Disasters, Nanjing University of Information Science & Technology, Nanjing, China
[3]National Climate Center, China Meteorological Administration (CMA), Beijing, China
[4]Key Laboratory of Tibetan Environment Changes and Land surface Processes, Institute of Tibetan Plateau Research, Chinese Academy of Sciences, Beijing, China
[5]State Key Laboratory of Loess and Quaternary Geology, Institute of Earth Environment, Chinese Academy of Sciences, Xi'an, China

Received: 24 April 2014 – Accepted: 10 May 2014 – Published: 21 May 2014

Correspondence to: J. Ming (petermingjing@hotmail.com)

Published by Copernicus Publications on behalf of the European Geosciences Union.

Abstract

The large change in albedo has a great effect on glacier ablation. Atmospheric aerosols (e.g. black carbon (BC) and dust) can reduce the albedo of glaciers and thus contribute to their melting. In this study, we investigated the measured albedo as well as the relationship between albedo and mass balance in Zhadang glacier on Mt. Nyanqentanglha associated with MODIS (10A1) data. The impacts of BC and dust in albedo reduction in different melting conditions were identified with SNow ICe Aerosol Radiative (SNICAR) model and in-situ data. It was founded that the mass balance of the glacier has a significant correlation with its surface albedo derived from Moderate Resolution Imaging Spectroradiometer (MODIS) onboard Terra satellite. The average albedo of Zhadang glacier from MODIS increased with the altitude and fluctuated but overall had a decreasing trend during 2001–2010, with the highest (0.722) in 2003 and the lowest (0.597) in 2009 and 2010, respectively. The sensitivity analysis via SNICAR showed that BC was a major factor in albedo reduction when the glacier was covered by newly fallen snow. Nevertheless, the contribution of dust to albedo reduction can be as high as 58 % when the glacier experienced strong surficial melting that the surface was almost bare ice. And the average radiative forcing (RF) caused by dust could increase from 1.1 to 8.6 $\mathrm{W\,m^{-2}}$ exceeding the forcings caused by BC after snow was deposited and surface melting occurred in Zhadang glacier. This suggest that it may be dust rather than BC, dominating the melting of some glaciers in the TP during melting seasons.

1 Introduction

Glaciers and snow cover are important reservoirs of fresh water on Earth. A rough volume of $2.4 \times 10^7\ \mathrm{km^3}$ of water is stored in them (Oki and Kanae, 2006) and changes in these reservoirs have a great effect on water supply in many regions of the world (Mote et al., 2003; Yao et al., 2012). The Tibetan Plateau (TP) is the source of many great rivers (e.g. Yangtze, Yellow, Indus, Ganges, and Brahmaputra rivers), which concentrate their sources at the glaciers in the TP known as the "Asian Water Towers". More than 1.4 billion people depend on the water from these rivers (Immerzeel et al., 2010), but these glaciers here have been undergoing rapid changes (Kang et al., 2010; Yao et al., 2012). Therefore, it is important to understand the impact factors that affect the glaciers and snow cover. The surface energy budget of glaciers has significant effects on their ablation (Zhang et al., 2013), and snow/ice albedo is one of the most important parameters that affect the absorbed radiation. Snow/ice albedo is defined as the fraction of the reflected and the incident radiant flux in the surface of the snow/ice. A higher albedo implies cleaner snow surface or less energy available for melting. Clean snow has the highest albedo (as high as 0.9) of any natural substance but this diminishes when snow surfaces are dirty or darkened (Warren and Wiscombe, 1980; Wiscombe and Warren, 1980). A recent report (Lhermitte et al., 2012) indicates a darkening surface of the Greenland ice sheet and a rapidly decreasing albedo during 2000–2011, which will greatly increase the rate of mass loss of the ice sheet as more solar energy is absorbed by the darker glacial ice (Farmer and Cook, 2013). It is widely recognized that temperature, precipitation and glacial dynamic processes are the key factors that affect glacial change (Sugden and John, 1976). However, there is now a general consensus that light-absorbing constituents (LACs, e.g. BC and dust) can reduce the albedo of glaciers (dirtying or darkening effect) and thus also contribute to the mass loss of glaciers. Both BC and dust are important absorbers of solar radiation in its visible spectra (Warren and Wiscombe, 1980; Hadley and Kirchstetter, 2012; IPCC, 2007), and BC has an absorbing capacity ~ 50 to 200 times higher than dust (Warren and Wiscombe, 1980). The impacts of BC and dust deposited on the TP glaciers (in particular, on their radiation balance) have been reported in the previous literatures (Ming et al., 2009a, 2013a). The simulation on the effect of LACs on the albedo of the Himalayan glaciers showed that LACs in this region had a contribution of 34 % to the albedo reduction during the spring time, with 21 % from BC, and 13 % originating from dust (Ming et al., 2012). The trend recorded over the last few decades has been that of declining albedo in the upper areas of most glaciers across the mid-Himalaya during the last decades; this phenomenon may be linked to BC and dust deposition on glacial surfaces during spring time (Ming et al., 2012). The lowering of surface albedo due to the presence of a dust layer could also lead to a drastic increase in the glacier melting rate during the melting season (Fujita, 2007). In general, BC can be transported over long distances (Ming et al., 2010), while dust usually comes from the local or regional environment of the glaciers (Kang et al., 2000). Historical deposition records of BC revealed by ice cores and lake sediments over the TP, indicate that BC originating from south and central Asia have inevitably reached the glaciers in recent decades (Ming et al., 2008; Xu et al., 2009b; Cong et al., 2013).

There has been extensive researches focusing on quantifying the impacts of LACs in ice cores and snow cover to understand the relationship between LACs and albedo reduction (Aoki et al., 2011; Painter et al., 2007, 2012; Ginot et al., 2013; Kaspari et al., 2013). However, few researchers discussed the exact effects that BC and dust take on different types of glacier surfaces during the melting season; Dust sometimes causes dramatic spatial variation of surface albedo in glaciers. Moreover, glacier melting causes LAC particles to concentrate in the surface and to further enhance absorbing the radiation. This positive feedback highlights the importance of investigating LACs and their effects on albedo and glacial melt across a whole glacier, particularly in a prevailing situation where glaciers are shrinking and emissions of BC are increasing (Bond et al., 2013). In this work, we investigate the spatial distribution of LACs from the terminate along to the accumulation zone of Zhadang glacier, southern TP during the summer of 2012 and estimate the contribution of BC and dust to the albedo reduction in different melting conditions.

2 Methodology

The Zhadang glacier is located in western Nyainqentanglha, southern TP, (30°28.57′ N, 90°38.71′ E, and 5500–5800 m a.s.l.) (Fig. 1). Surface snow/ice samples were collected and surface albedo was observed on Zhadang glacier during 12–16 July and 24–27

August 2012. We classified three conditions or scenarios of the glacier surface: (1) S-I: the surface of the glacier is bare ice containing some visible dark constituents (Fig. 2a); (2) S-II: the surface is covered by aged snow/firn (Fig. 2a); (3) S-III: the surface is covered by fresh snow (Fig. 2b). These surface conditions are typical in most alpine glaciers all around the year (Benn and Evans, 2010). The description of sampling details in Zhadang glacier is given in Table 1.

2.1 Albedo data from the Moderate Resolution Imaging Spectroradiometer (MODIS) onboard Terra

The MODIS albedo data were used to investigate the albedo change in Zhandang glacier. The series of the product is MODIS/Terra Snow Cover Daily L3 Global 500 m Grid (MOD10A1), which are based on a snow mapping algorithm that employs a normalized difference snow index (NDSI) and other criteria tests (Riggs and Hall, 2011). MOD10A1 product contains four data layers: snow cover, snow albedo, fractional snow cover, and quality assessment (QA). They are compressed in hierarchical data format-Earth observing system (HDF-EOS) formatted along with corresponding metadata. The images of MOD10A1 are 1200 km by 1200 km tiles with a resolution of 500 m × 500 m gridded in a sinusoidal map projection. Data are available from 24 February 2000 to present via FTP (Hall et al., 2006). The snow albedo data that used to calculate are based on three criteria below: the pixels are identified as snow cover, fractional snow cover is 100, and the pixels pass the QA. MODIS daily albedo has high accuracy in flat terrain (Stroeve et al., 2006; Tekeli et al., 2006.), while it shows some errors in complex topography such as mountainous regions (Sorman et al., 2007; Warren, 2013). In order to verify the applicability of MOD10A1 product in Zhadang glacier, we use the observed data measured by the Kipp & Zonen radiometers mounted on an automatic weather station (AWS), which was set in the saddle of the glacier (5680 m a.s.l., Fig. 1). The albedo data was extracted from the precise pixel in the relevant MODIS image where the AWS located. The observed albedo were selected in the local time period of 12:30 to 13:30 LT, considering the right scanning time of Terra satellite passing over the study area. The correlation analysis between the MODIS data and observed data showed a good relationship at the confidence level of 0.02 (Fig. 3), indicating that it is reasonable to use MOD10A1 data to study to albedo change of Zhadang glacier.

2.2 Field albedo observation

A spectroradiometer (Model ASD® FS-3) was used to measure the spectral albedo of the glacier. This covers a radiation waveband of 350–2500 nm with a wavelength resolution of one nanometre. The optical sensor of the spectroradiometer was mounted in a pistol-shape unit and fixed at the height of approximately 0.5 m above the snow/ice surface to measure spectral reflectance. During the expedition of July 2012, we measured surface albedo and collected snow/ice samples in S-I (two sites: A and B) and S-II (C and D) conditions. In August, the glacier was covered by newly fallen snow, and albedo and surface snow samples were successfully observed and collected at eight sites in S-III condition (Fig. 2). Along with the sampling, other necessary parameters such as snow density, grain sizes, and etc. for simulating the surface albedo were also observed. Details concerning the simulations of surface albedo have been introduced in a previous work (Ming et al., 2013a).

2.3 Snow/ice sampling and BC/dust measurement

Snow/ice samples were collected in accordance with the “Clean hands-Dirty Hands” principle (Fitzgerald, 1999). We collected two parallel samples 10 cm away from each other from surface to 5 cm depth at each site when measuring albedo. Snow density was measured using a balance. The samples were stored in NALGENE® HDPE wide-mouth bottles (250 mL) and kept in frozen condition until laboratory analysis. The snow grain sizes were measured using a hand lens (25×) with accuracy of 0.02 mm; the largest length of a single ice crystal was also measured using a snow crystal card with 1 mm grids (Aoki et al., 2007). We filtered the snow melt water through quartz-fiber filters, which were weighed before and after the filtration using a microbalance to evaluate the mass of on-load dust. A thermal-optical method of carbon analysis, using DRI® Model 2001A OC/EC (Chow et al., 1993) was employed to measure BC mass in the samples.

2.4 Albedo reduction modelling and radiative forcing (RF)

The SNow ICe Aerosol Radiative (SNICAR) model can be used to simulate the hemisphere albedo of snow and ice for unique combinations of impurity contents (BC, dust, and volcanic ash), snow size, and incident solar flux characteristics (Flanner et al., 2007). It was applied to simulate the albedo varying caused by BC and dust deposited in the glacier surface in this work. We conducted a series of sensitivity analysis to identify the impact of BC and dust on albedo reduction in three different surface conditions of Zhadang glacier (also see Sect. 2.2). Solar zenith angle was identified based on the time and position of specific sampling sites. Snow grain effective radius is taken as the half of observed snow grain size shown in Table 1. The albedo of the underlying ground is taken as 0.11–0.19 in the visible band and 0.18–0.23 in the near-infrared band, based on observations. The mass absorption cross-section (MAC) of BC was set as 11, which is the median of typical MAC values (Hadley and Kirchstetter, 2012). The detailed parameters used in SNICAR are listed in the appendix.

RF was defined using the equation below,

$$\mathrm{RF} = R_{\text{in-short}} \cdot \Delta\alpha,$$

where $R_{\text{in-short}}$ denotes incident solar radiation measured by radiometer, and $\Delta\alpha$ denotes the reduction of albedo.

3 Results and discussions

3.1 Surface albedo variations of Zhadang glacier into the 21st century

The albedo of Zhadang glacier increased with elevation (Table 1) due to the lower temperature favouring more cold snow stored in higher elevations. The MODIS albedo of Zhadang glacier shows an obvious decreasing trend of 0.0010 a^{-1} during 2001–2010, in spite of the inter-annual fluctuations (Fig. 4). The annually average albedo declined from 0.676 in 2001 to 0.597 in 2010 with a maximum of 0.722 in 2003, and a minimum of 0.597 in 2009 and 2010. This trend was also revealed in the Himalayan and Tanggula glaciers (Ming et al., 2012; Wang et al., 2012).

Surface albedo of a specific glacier could be linked with its mass balance in the TP, which has been proved by Wang et al. (2013). We used the observed mass balance data from 2006 through 2010 in Zhadang glacier (Zhang et al., 2013) and did a correlation analysis with the glacier surface albedo (Fig. 4). Lower albedo is relative to larger negative balances, and vice versa. For example, the most negative mass balance of Zhadang glacier was appearing in 2010 when the albedo of the glacier reaches to the minimum, whereas the positive mass balance occurred in 2008 and the albedo was the highest during 2006–2010. The significant positive correlation ($n = 6$, $\alpha = 0.01$, $R^2 > 0.95$) between albedo and the mass balance of the glacier indicates that the surface albedo of Zhadang glacier can be a strong index of glacier mass balance.

3.2 Impacts of BC and dust on albedo

BC and dust concentrations, as well as other observations such as snow grain size, snowpack density, snowpack thickness, and etc., on Zhadang glacier are shown in Table 1. In S-I condition, the concentration of dust varied from 504–1892 ppm with an average of 1198 ppm, while BC was 334–473 ppb with an average of 404 ppb. The concentration of BC here is much higher than those recorded in previous observations in the Arctic, Antarctic, Greenland and China (Ye et al., 2012; Ming et al., 2009b; Xu et al., 2012, 2009a, b; Weller et al., 2013; McConnell et al., 2012; Bisiaux et al., 2012; Dou et al., 2012; Wang et al., 2011; Gong et al., 2010). In S-II condition, the concentrations of BC and dust ranged from 81 to 143 ppb with an average of 112 ppb, and 34 to 67 ppm with an average of 50 ppm, respectively. However, the concentration of BC in S-III was 41 to 59 ppb with an average of 52 ppb, while the dust concentration was 3 to 8 ppm with an average of 6 ppm. There are large differences in BC and dust concentrations in the surface of Zhadang glacier in different scenarios of surface features (Fig. 2a). In S-I and S-II, intensive surface melting could lead to a strong enrichment of LACs in the surface of the glacier. In S-III conditions, Zhadang glacier was covered by fresh snow due to frequent snowfalls at nights (Fig. 2b). Thus, the concentrations of LACs in S-III are several magnitudes lower than those in S-I and S-II conditions (Table 1). Table 2 provides observed and simulated albedo at the sampling sites. The observed surface albedo increases along with elevations on Zhadang glacier, in contrast with the concentrations of BC and dust in S-I and S-II conditions. This suggests that the enrichment of BC and dust on the surface of the glacier could reduce the glacier albedo, thus resulting in melting of glaciers.

The sensitivity analysis of the respective impacts of BC and dust on reducing snow albedo of Zhadang glacier was showed in Fig. 5. We presume three impacting factors dominating the albedo varying in the glacial surface, i.e., BC, dust, and the grain size growing due to warming (Ming et al., 2012). Dust exceeding BC was the most dominant factor of reducing glacier albedo in S-I. BC other than dust dominates reducing albedo in case the glacier was covered by snow (S-II and S-III). The incoming solar irradiances at every sampling time during the two trips are listed in Table 2. We calculated the RF of both BC and dust on the Zhadang glacier. The simulation shows that the RF caused by BC and dust deposition on Zhadang glacier varied between 0.4–11.8 $\mathrm{W\,m^{-2}}$ and 0.5–16.4 $\mathrm{W\,m^{-2}}$, respectively (Fig. 5). The RF of dust is much higher than that of BC in S-I, while the RF of BC exceeds dust in S-II and S-III. On average, the forcing caused by dust deposition on the Zhadang glacier in the summer of 2012 was $2.7 \pm 3.4\ \mathrm{W\,m^{-2}}$, and that caused by BC was $4.8 \pm 3.2\ \mathrm{W\,m^{-2}}$, which is a little lower than that recorded in the northern TP (Ming et al., 2013b), and higher than those recorded in the Arctic (Flanner, 2013; Dou et al., 2012).

4 Summary and conclusions

The albedo of Zhadang glacier had been declining during the 10 years of 2001–2010 suggested by MODIS data and has a significant correlation with the mass balance. That means remotely sensed albedo data could be used in the research of mass balance change of glacier in large spatial scale. During the summer of 2012, the average concentrations of BC and dust are 404 and 1198 ppm in the surface of Zhadang glacier, which were one and three magnitudes higher than 52 ppb of BC and 6.4 ppm of dust in fresh snow. The effects of BC and dust on the glacier albedo were quantified based both on observed and simulated data. The contribution of dust and BC to albedo reduction was 58 and 27 %, respectively, when the glacier was covered by bare ice. In the surface covered by aged snow, 36 % of the surface albedo reduction was caused by BC, and 29 % was caused by dust, respectively. When the glacier was covered by fresh snow, BC and dust contributed 12 and 3 % to albedo decreasing, respectively. BC was a major factor inducing albedo decreasing when the glacier was covered by snow including the fresh and aged. Dust made the most significant contribution to albedo reduction when the glacier was bare-ice covered.

Acknowledgements. This work was supported by the Global Change Research Program of China (2010CB951401), the National Natural Science Foundation of China (Grants 41121001, 41225002, and 41190081), State Key Laboratory of Cryospheric Sciences, CAS (no. SKLCS-ZZ-2012-01-06), CMA (no. GYHY201106023), and the Climate Change Science Foundation of CMA (2013–2014). The authors would like to give thanks to H. Zhang for his great help on processing the albedo data.

References

Aoki, T., Hori, M., Motoyoshi, H., Tanikawa, T., Hachikubo, A., Sugiura, K., Yasunari, T. J., Storvold, R., Eide, H. A., and Stamnes, K.: ADEOS-II/GLI snow/ice products – Part II: Validation results using GLI and MODIS data, Remote Sens. Environ., 111, 274–290, doi:10.1016/j.rse.2007.02.035, 2007.

Aoki, T., Kuchiki, K., Niwano, M., Kodama, Y., Hosaka, M., and Tanaka, T.: Physically based snow albedo model for calculating broadband albedos and the solar heating profile in snowpack for general circulation models, J. Geophys. Res.-Atmos., 116, D11114, doi:10.1029/2010jd015507, 2011.

Benn, D. I. and Evans, D. J.: Glaciers and Glaciation, Hodder Education, London, 2010.

Bisiaux, M. M., Edwards, R., McConnell, J. R., Albert, M. R., Anschütz, H., Neumann, T. A., Isaksson, E., and Penner, J. E.: Variability of black carbon deposition to the East Antarctic Plateau, 1800–2000 AD, Atmos. Chem. Phys., 12, 3799–3808, doi:10.5194/acp-12-3799-2012, 2012.

Bond, T., Doherty, S., Fahey, D., Forster, P., Berntsen, T., DeAngelo, B., Flanner, M., Ghan, S., Kärcher, B., and Koch, D.: Bounding the role of black carbon in the climate system: a scientific assessment, J. Geophys. Res.-Atmos., 118, 5380–5552, doi:10.1002/jgrd.50171, 2013.

Chow, J. C., Watson, J. G., Pritchett, L. C., Pierson, W. R., Frazier, C. A., and Purcell, R. G.: The DRI thermal/optical reflectance carbon analysis system: description, evaluation and applications in US air quality studies, Atmos. Environ. A-Gen., 27, 1185–1201, 1993.

Cong, Z., Kang, S., Gao, S., Zhang, Y., Li, Q., and Kawamura, K.: Historical trends of atmospheric black carbon on Tibetan Plateau as reconstructed from a 150-year lake sediment record, Environ. Sci. Technol., 47, 2579–2586, doi:10.1021/es3048202, 2013.

Dou, T., Xiao, C., Shindell, D. T., Liu, J., Eleftheriadis, K., Ming, J., and Qin, D.: The distribution of snow black carbon observed in the Arctic and compared to the GISS-PUCCINI model, Atmos. Chem. Phys., 12, 7995–8007, doi:10.5194/acp-12-7995-2012, 2012.

Farmer, G. T. and Cook, J.: Earth's albedo, radiative forcing and climate change, in: Climate Change Science: a Modern Synthesis, Springer, the Netherlands, 217–229, 2013.

Fitzgerald, W. F.: Clean hands, dirty hands: Clair Patterson and the aquatic biogeochemistry of mercury, in: Clean Hands, Clair Patterson's Crusade Against Environmental Lead Contamination, Nova Science Publishers, Commack, NY, 119–137, 1999.

Flanner, M. G.: Arctic climate sensitivity to local black carbon, J. Geophys. Res.-Atmos., 118, 1840–1851, doi:10.1002/jgrd.50176, 2013.

Flanner, M. G., Zender, C. S., Randerson, J. T., and Rasch, P. J.: Present-day climate forcing and response from black carbon in snow, J. Geophys. Res., 112, D11202, doi:10.1029/2006JD008003, 2007.

Fujita, K.: Effect of dust event timing on glacier runoff: sensitivity analysis for a Tibetan glacier, Hydrol. Process., 21, 2892–2896, 2007.

Ginot, P., Dumont, M., Lim, S., Patris, N., Taupin, J.-D., Wagnon, P., Gilbert, A., Arnaud, Y., Marinoni, A., Bonasoni, P., and Laj, P.: A 10 yr record of black carbon and dust from Mera Peak ice core (Nepal): variability and potential impact on Himalayan glacier melting, The Cryosphere Discuss., 7, 6001–6042, doi:10.5194/tcd-7-6001-2013, 2013.

Gong, S., Zhao, T., Sharma, S., Toom-Sauntry, D., Lavoué, D., Zhang, X., Leaitch, W., and Barrie, L.: Identification of trends and interannual variability of sulfate and black carbon in the Canadian High Arctic: 1981–2007, J. Geophys. Res., 115, D07305, doi:10.1029/2009JD012943, 2010.

Hadley, O. L. and Kirchstetter, T. W.: Black-carbon reduction of snow albedo, Nature Climate Change, 2, 437–440, 2012.

Hall, D. K., Riggs, G. A., and Salomonson, V. V.: MODIS/Terra Snow Cover Daily L3 Global 500 m Grid V005, (January 2001 to December 2010), National Snow and Ice Data Center, Boulder, Colorado, USA, Digital media (updated daily), 2006.

Immerzeel, W. W., van Beek, L. P., and Bierkens, M. F.: Climate change will affect the Asian water towers, Science, 328, 1382–1385, 2010.

IPCC Climate Change 2007: The Physical Science Basis Contribution of Working Group I to the Fourth Assessment Report of the Intergovernmental Panel on Climate Change, edited by: Solomon, S., Qin, D., Manning, M., Chen, Z., Marquis, M., Averyt, K. B., Tignor, M., and Miller, H. L., Cambridge University Press, Cambridge, UK and New York, NY, USA, 996 pp., 2007.

Kang, S., Wake, C. P., Dahe, Q., Mayewski, P. A., and Tandong, Y.: Monsoon and dust signals recorded in Dasuopu glacier, Tibetan Plateau, J. Glaciol., 46, 222–226, 2000.

Kang, S., Xu, Y., You, Q., Flügel, W. A., Pepin, N., and Yao, T.: Review of climate and cryospheric change in the Tibetan Plateau, Environ. Res. Lett., 5, 015101, doi:10.1088/1748-9326/5/1/015101, 2010.

Kaspari, S., Painter, T. H., Gysel, M., and Schwikowski, M.: Seasonal and elevational variations of black carbon and dust in snow and ice in the Solu-Khumbu, Nepal and estimated radiative forcings, Atmos. Chem. Phys. Discuss., 13, 33491–33521, doi:10.5194/acpd-13-33491-2013, 2013.

Lhermitte, S., Greuell, W., van Meijgaard, E., van Oss, R., van den Broeke, M., and van de Berg, W.: Greenland ice sheet surface albedo: trends in surface properties (2000–2011), EGU General Assembly Conference Abstracts, 12349, 2012.

McConnell, J. R., Sigl, M., Baggenstos, D., Fritzsche, D., Dahl-Jensen, D., Das, S., Kreutz, K., Maselli, O., McGwire, K. C., Nolan, M., Opel, T., Severinghaus, J., and Steffensen, J. P.: Black carbon concentrations and fluxes since the Last Glacial Maximum in Greenland and Antarctic ice cores, AGU Fall Meeting, San Francisco, Calif., USA, 3–7 December 2012.

Ming, J., Cachier, H., Xiao, C., Qin, D., Kang, S., Hou, S., and Xu, J.: Black carbon record based on a shallow Himalayan ice core and its climatic implications, Atmos. Chem. Phys., 8, 1343–1352, doi:10.5194/acp-8-1343-2008, 2008.

Ming, J., Xiao, C., Du, Z., and Flanner, M. G.: Black Carbon in snow/ice of west China and its radiave forcing, Advances in Climate Change Research, 92, 114–123, 2009a.

Ming, J., Xiao, C. D., Cachier, H., Qin, D. H., Qin, X., Li, Z. Q., and Pu, J. C.: Black Carbon (BC) in the snow of glaciers in west China and its potential effects on albedos, Atmos. Res., 92, 114–123, 2009b.

Ming, J., Xiao, C., Sun, J., Kang, S., and Bonasoni, P.: Carbonaceous particles in the atmosphere and precipitation of the Nam Co region, central Tibet, J. Environ. Sci., 22, 1748–1756, 2010.

Ming, J., Du, Z., Xiao, C., Xu, X., and Zhang, D.: Darkening of the mid-Himalaya glaciers since 2000 and the potential causes, Environ. Res. Lett., 7, 014021, doi:10.1088/1748-9326/7/1/014021, 2012.

Ming, J., Wang, P., Zhao, S., and Chen, P.: Disturbance of light-absorbing aerosols on the albedo in a winter snowpack of Central Tibet, J. Environ. Sci., 337, 1601–1607, 2013a.

Ming, J., Xiao, C., Du, Z., and Yang, X.: An overview of black carbon deposition in high Asia Glaciers and its impacts on radiation balance, Adv. Water Resour., 55, 80–87, 2013b.

Mote, P. W., Parson, E. A., Hamlet, A. F., Keeton, W. S., Lettenmaier, D., Mantua, N., Miles, E. L., Peterson, D. W., Peterson, D. L., and Slaughter, R.: Preparing for climatic change: the water, salmon, and forests of the Pacific Northwest, Climatic Change, 61, 45–88, 2003.

Oki, T. and Kanae, S.: Global hydrological cycles and world water resources, Science, 313, 1068–1072, 2006.

Painter, T. H., Barrett, A. P., Landry, C. C., Neff, J. C., Cassidy, M. P., Lawrence, C. R., McBride, K. E., and Farmer, G. L.: Impact of disturbed desert soils on duration of mountain snow cover, Geophys. Res. Lett., 34, L12502, doi:10.1029/2007GL030284, 2007.

Painter, T. H., Skiles, S. M., Deems, J. S., Bryant, A. C., and Landry, C. C.: Dust radiative forcing in snow of the Upper Colorado River Basin: 1. A 6 year record of energy balance, radiation, and dust concentrations, Water Resour. Res., 48, W07521, doi:10.1029/2012WR011985, 2012.

Riggs, G. and Hall, D.: MODIS snow and ice products, and their assessment and applications, in: Land Remote Sensing and Global Environmental Change, Springer, New York, 681–707, 2011.

Şorman, A. Ü., Akyürek, Z., Şensoy, A., Şorman, A. A., and Tekeli, A. E.: Commentary on comparison of MODIS snow cover and albedo products with ground observations over the mountainous terrain of Turkey, Hydrol. Earth Syst. Sci., 11, 1353–1360, doi:10.5194/hess-11-1353-2007, 2007.

Stroeve, J. C., Box, J. E., and Haran, T.: Evaluation of the MODIS (MOD10A1) daily snow albedo product over the Greenland ice sheet, Remote Sens. Environ., 105, 155–171, 2006.

Sugden, D. E. and John, B. S.: Glaciers and Landscape: a Geomorphological Approach, Edward Arnold, London, 1976.

Tekeli, A. E., Şensoy, A., Şorman, A., Akyürek, Z., and Şorman, Ü.: Accuracy assessment of MODIS daily snow albedo retrievals with in situ measurements in Karasu basin, Turkey, Hydrol. Process., 20, 705–721, 2006.

Wang, J., Ye, B., Cui, Y., He, X., and Yang, G.: Spatial and temporal variations of albedo on nine glaciers in western China from 2000 to 2011, Hydrol. Process., 28, 3454–3465, doi:10.1002/hyp.9883, 2013.

Wang, Q., Jacob, D. J., Fisher, J. A., Mao, J., Leibensperger, E. M., Carouge, C. C., Le Sager, P., Kondo, Y., Jimenez, J. L., Cubison, M. J., and Doherty, S. J.: Sources of carbonaceous aerosols and deposited black carbon in the Arctic in winter-spring: implications for radiative forcing, Atmos. Chem. Phys., 11, 12453–12473, doi:10.5194/acp-11-12453-2011, 2011.

Warren, S. G.: Can black carbon in snow be detected by remote sensing?, J. Geophys. Res.-Atmos., 118, 779–786, 2013.

Warren, S. G. and Wiscombe, W. J.: A model for the spectral albedo of snow. II: Snow containing atmospheric aerosols, J. Atmos. Sci., 37, 2734–2745, 1980a.

Wiscombe, W. J. and Warren, S. G.: A model for the spectral albedo of snow. I: Pure snow, J. Atmos. Sci., 37, 2712–2733, 1980b.

Weller, R., Minikin, A., Petzold, A., Wagenbach, D., and König-Langlo, G.: Characterization of long-term and seasonal variations of black carbon (BC) concentrations at Neumayer, Antarctica, Atmos. Chem. Phys., 13, 1579–1590, doi:10.5194/acp-13-1579-2013, 2013.

Xu, B., Cao, J., Hansen, J., Yao, T., Joswia, D. R., Wang, N., Wu, G., Wang, M., Zhao, H., and Yang, W.: Black soot and the survival of Tibetan glaciers, P. Natl. Acad. Sci. USA, 106, 22114–22118, 2009a.

Xu, B., Wang, M., Joswiak, D. R., Cao, J. J., Yao, T. D., Wu, G. J., Yang, W., and Zhao, H. B.: Deposition of anthropogenic aerosols in a southeastern Tibetan glacier, J. Geophys. Res., 114, D17209, doi:10.1029/2008JD011510, 2009b.

Xu, B., Cao, J., Joswiak, D. R., Liu, X., Zhao, H., and He, J.: Post-depositional enrichment of black soot in snow-pack and accelerated melting of Tibetan glaciers, Environ. Res. Lett., 7, 014022, doi:10.1088/1748-9326/7/1/014022, 2012.

Yao, T., Thompson, L., Yang, W., Yu, W., Gao, Y., Guo, X., Yang, X., Duan, K., Zhao, H., and Xu, B.: Different glacier status with atmospheric circulations in Tibetan Plateau and surroundings, Nature Climate Change, 2, 663–667, 2012.

Ye, H., Zhang, R., Shi, J., Huang, J., Warren, S. G., and Fu, Q.: Black carbon in seasonal snow across northern Xinjiang in northwestern China, Environ. Res. Lett., 7, 044002, doi:10.1088/1748-9326/7/4/044002, 2012.

Zhang, G., Kang, S., Fujita, K., Huintjes, E., Xu, J., Yamazaki, T., Haginoya, S., Wei, Y., Scherer, D., and Schneider, C.: Energy and mass balance of Zhadang glacier surface, central Tibetan Plateau, J. Glaciol., 59, 137–148, 2013.

Table 1. Sampling information: two expeditions were conducted in Zhadang glacier and samples (albedo, snow/ice) were collected under three melting conditions of the glacier, in July and August of 2012. We measured the albedo five to six times at each site whilst collecting two to three snow/ice samples. In total, 120 albedo measurements and 48 snow/ice samples were obtained at the A–D sample site in July 2012 for S-I and S-II conditinos (Fig. 2). A total of 160 albedo samples and 64 snow samples were obtained at all sampling sites in August 2012. The albedo and concentrations of BC and dust are listed here.

Sample date	Sample site	Altitude (m a.s.l.)	Number of samples (albedo/ snow and ice)	Average of albedo	Average of BC conc. (ppb)	Average of dust conc. (ppm)	Snow grain size (mm)	Snowpack density (kg m^{-3})	Snowpack thickness (cm)	Solar zenith angle (°)	Cloud amount (10 = 100 %)	Scene type
Jul 2012	A	5507	30/12	0.385	472.6	503.8	0.8 ~ 1.6	289 ~ 380	1	44.8 ~ 78.9	3 ~ 10	S-I
	B	5680	30/12	0.521	334.4	1891.9	0.6 ~ 1.6	289 ~ 350	1 ~ 2	52.3 ~ 75.8	1 ~ 10	
	C	5720	30/12	0.676	142.9	66.6	0.4 ~ 0.7	333 ~ 378	2 ~ 3	62.9 ~ 79.1	1 ~ 10	S-II
	D	5795	30/12	0.686	80.9	33.6	0.3 ~ 0.5	267 ~ 289	3	67.1 ~ 67.3	0 ~ 10	
Aug 2012	A	5507	20/8	0.589	53.2	8.2	0.2 ~ 0.5	278 ~ 300	1 ~ 2	33.4 ~ 44	0 ~ 10	S-III
	B	5560	20/8	0.696	40.8	8.0	0.2 ~ 0.4	256 ~ 289	2 ~ 3	37.6 ~ 47.1	1 ~ 7	
	C	5626	20/8	0.710	55.5	7.0	0.2 ~ 0.4	267 ~ 311	2 ~ 3	40.8 ~ 50.2	0 ~ 7	
	D	5680	20/8	0.699	52.7	6.7	0.2 ~ 0.4	267 ~ 289	3	43.8 ~ 54.1	1 ~ 8	
	E	5695	20/8	0.708	55.2	6.4	0.2 ~ 0.4	267 ~ 289	3 ~ 4	45.8 ~ 57.9	0 ~ 6	
	F	5715	20/8	0.667	57.7	6.2	0.2 ~ 0.4	278 ~ 289	4	49.9 ~ 61.4	0 ~ 7	
	G	5750	20/8	0.698	59.4	5.2	0.2 ~ 0.3	222 ~ 244	5	51.9 ~ 64.6	0 ~ 7	
	H	5795	20/8	0.724	40.9	3.4	0.2 ~ 0.3	211 ~ 222	5	61.2 ~ 68.4	0 ~ 10	

Table 2. Sensitivity analysis with SNICAR model. BC % and dust % are the contribution of BC and dust to the total reduction of albedo, respectively. $R_{\text{in-short}}$ is the incident solar radiation measured by AWS.

Date	Site	OA[a]	SA[b] pure	SA + BC	SA + BC and dust	BC %	dust %	$R_{\text{in-short}}$	RF + BC	RF + dust	Scene type
15 Jul	A	0.385	0.406	0.395	0.388	52	33	780.1	8.6	5.5	S-I
16 Jul	A	0.387	0.410	0.405	0.395	22	44	412.6	2.1	4.1	
15 Jul	B	0.363	0.406	0.394	0.364	28	70	548.2	6.6	16.4	
16 Jul	B	0.558	0.577	0.576	0.560	4	85	535.3	0.4	8.6	
14 Jul	C	0.618	0.640	0.631	0.624	41	32	1308.5	11.8	9.2	S-II
15 Jul	C	0.723	0.758	0.742	0.727	46	43	543.7	8.7	8.2	
16, Jul	C	0.745	0.756	0.754	0.752	18	18	604.4	1.2	1.2	
14 Jul	D	0.745	0.771	0.760	0.753	42	27	552.7	6.1	3.9	
15 Jul	D	0.732	0.754	0.745	0.740	41	23	648.4	5.8	3.2	
16 Jul	D	0.755	0.775	0.770	0.764	25	30	789.8	3.9	4.7	
24 Aug	A	0.568	0.790	0.786	0.784	2	1	337.8	1.4	0.7	
25 Aug	A	0.653	0.682	0.681	0.680	5	2	658.7	0.9	0.5	S-III
26 Aug	A	0.716	0.746	0.739	0.737	23	7	702.5	4.9	1.4	
24 Aug	B	0.759	0.793	0.779	0.778	41	4	608.1	8.5	0.9	
25 Aug	B	0.696	0.731	0.728	0.727	8	4	722.7	1.9	0.9	
26 Aug	B	0.656	0.683	0.681	0.68	7	4	736.2	1.5	0.7	
24 Aug	C	0.772	0.799	0.789	0.787	37	7	1162	11.6	2.3	
25 Aug	C	0.794	0.819	0.816	0.815	12	4	768.3	2.3	0.8	
26 Aug	C	0.697	0.734	0.732	0.732	5	1	776.8	1.6	0.3	
24 Aug	D	0.726	0.806	0.797	0.795	11	3	822.6	7.4	1.6	
25 Aug	D	0.768	0.781	0.780	0.778	17	10	814	1.8	1.1	
26 Aug	D	0.647	0.781	0.779	0.778	1	1	811	1.3	1.0	
24 Aug	E	0.699	0.810	0.803	0.802	6	1	962	6.7	1.0	
25 Aug	E	0.780	0.813	0.809	0.807	12	6	891.5	3.6	1.8	
26 Aug	E	0.774	0.811	0.805	0.804	16	3	831	5.0	1.0	
24 Aug	F	0.792	0.839	0.835	0.833	9	4	786.8	3.1	1.6	
25 Aug	F	0.790	0.819	0.816	0.815	10	3	1030	3.1	1.0	
26 Aug	F	0.566	0.816	0.809	0.808	3	1	895	6.0	1.2	
24 Aug	G	0.795	0.848	0.840	0.838	15	4	1303	10.4	2.6	
25 Aug	G	0.806	0.828	0.824	0.823	18	5	1168	4.7	1.2	
26 Aug	G	0.652	0.819	0.812	0.811	4	1	932	6.5	0.9	
24 Aug	H	0.811	0.853	0.846	0.846	16	1	1134	7.5	0.6	
25 Aug	H	0.809	0.834	0.831	0.830	12	4	1316	3.9	1.3	
26 Aug	H	0.711	0.827	0.825	0.824	2	1	1192	2.4	1.2	
Avg.	S-I,II,III	0.690	0.745	0.739	0.735	18	14	826.1	4.8	2.7	

[a] OA denotes observed abedo.

[b] SA denotes simulated albedo.

Table A1. Parameters for sensitivity analysis with SNICAR. 1. Incident radiation (a. Direct, b. Diffuse); 2. Solar zenith angle; 3. Surface spectral distribution (a. Mid-latitude winter, clear-sky, cloud amount < 5. b. Mid-latitude winter, cloudy, cloud amount ≥ 5); 4. Snow grain effective radius (µm); 5. Snowpack thickness (m); 6. Snowpack density (kg m^{-3}); 7. Albedo of underlying ground (a. Visible, 0.3–0.7 µm. b. Near-infrared, 0.7–5.0 µm); 8. MAC scaling factor (experimental) for BC; 9. Black carbon concentration (ppb, Sulfate-coated); 10. Dust concentration (ppm, 5.0–10.0 µm diameter); 11. Volcanic ash concentration (ppm); 12. Experimental particle 1 concentration (ppb).

Date	site	1	2	3	4	5	6	7a	7b	8	9	10	11	12
14 Jul	C	b	79.1	b	600	0.02	378	0.15	0.3	11	129.9	56.4	0	0
14 Jul	D	b	67.3	b	400	0.05	289	0.15	0.3	11	77.2	29.6	0	0
15 Jul	A	b	78.9	b	800	0.01	289	0.13	0.12	11	608.2	649.3	0	0
15 Jul	B	b	75.8	b	800	0.01	289	0.13	0.12	11	657.3	3628.8	0	0
15 Jul	C	a	71.6	a	400	0.02	367	0.15	0.3	11	278	135.1	0	0
15 Jul	D	a	67.2	a	400	0.03	278	0.15	0.3	11	114	39	0	0
16 Jul	A	a	44.8	a	700	0.01	380	0.13	0.12	11	337	358.3	0	0
16 Jul	B	a	52.3	a	700	0.02	350	0.15	0.3	11	11.5	155	0	0
16 Jul	C	a	62.9	b	400	0.03	333	0.15	0.3	11	20.8	8.3	0	0
16 Jul	D	a	67.1	a	400	0.04	267	0.15	0.3	11	51.5	32.2	0	0
24 Aug	A	b	44	b	250	0.03	300	0.13	0.12	11	60.2	9.6	0	0
24 Aug	B	a	47.1	b	200	0.03	289	0.13	0.12	11	153.6	8.2	0	0
24 Aug	C	a	50.2	b	200	0.02	311	0.13	0.12	11	111.4	9	0	0
24 Aug	D	a	54.1	a	200	0.03	289	0.13	0.12	11	115.4	8.1	0	0
24 Aug	E	a	57.9	a	200	0.03	267	0.15	0.3	11	87.6	7.7	0	0
24 Aug	F	a	61.4	a	200	0.04	289	0.15	0.3	11	41.3	9.1	0	0
24 Aug	G	a	64.6	b	200	0.05	244	0.15	0.3	11	84.7	7.1	0	0
24 Aug	H	a	68.4	b	200	0.05	222	0.15	0.3	11	67.9	2.6	0	0
25 Aug	A	a	33.4	a	250	0.02	278	0.13	0.12	11	29.2	5.9	0	0
25 Aug	B	a	37.6	a	200	0.02	278	0.13	0.12	11	43.2	9.1	0	0
25 Aug	C	a	40.8	b	200	0.03	311	0.13	0.12	11	32.2	6.1	0	0
25 Aug	D	a	43.9	b	200	0.03	267	0.13	0.12	11	22.5	6.8	0	0
25 Aug	E	a	47	b	200	0.04	289	0.15	0.3	11	31.4	6.3	0	0
25 Aug	F	a	52	b	200	0.04	278	0.15	0.3	11	28.3	4.1	0	0
25 Aug	G	a	54	b	200	0.05	244	0.15	0.3	11	33.4	3.2	0	0
25 Aug	H	a	61.2	b	200	0.05	211	0.15	0.3	11	33.6	5.6	0	0
26 Aug	A	a	37.5	b	250	0.03	289	0.13	0.12	11	70.2	9.2	0	0
26 Aug	B	a	39.6	a	250	0.02	256	0.13	0.12	11	38.3	6.8	0	0
26 Aug	C	a	41.7	b	200	0.02	267	0.13	0.12	11	23	5.9	0	0
26 Aug	D	a	43.8	a	200	0.03	267	0.13	0.12	11	20.3	5.2	0	0
26 Aug	E	a	45.8	b	200	0.04	289	0.15	0.3	11	46.6	5.2	0	0
26 Aug	F	a	49.9	b	200	0.04	278	0.15	0.3	11	57.7	5.5	0	0
26 Aug	G	a	51.9	b	200	0.05	222	0.15	0.3	11	60	5.4	0	0
26 Aug	H	b	62.6	b	200	0.05	211	0.15	0.3	11	21.1	2.1	0	0

SNICAR online, http://snow.engin.umich.edu/

Title Page
Abstract | Introduction
Conclusions | References
Tables | Figures
◀▶
Back | Close
Full Screen / Esc
Printer-friendly Version
Interactive Discussion

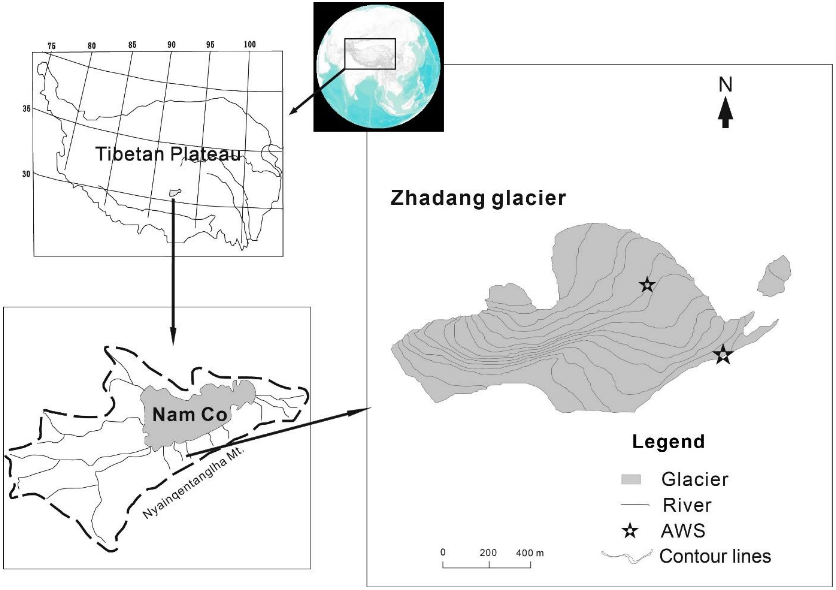

Figure 1. Location of Zhangdang glacier on Mt. Nyainqentanglha.

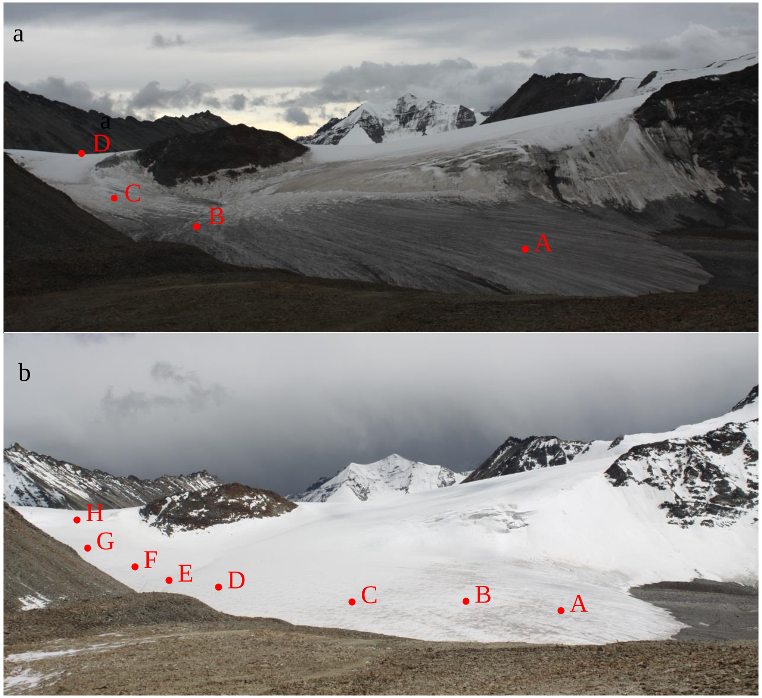

Figure 2. Surface features of Zhadang glacier on 16 July **(a)** and 26 August **(b)**. The two surface conditions include three types of melting scenes: S-I: Sites A and B which are located in the superimposed ice belt **(a)**; S-II: Sites C and D which are in the upper area of the glacier **(a)**; S-III: All sites were covered by fresh snow **(b)**.

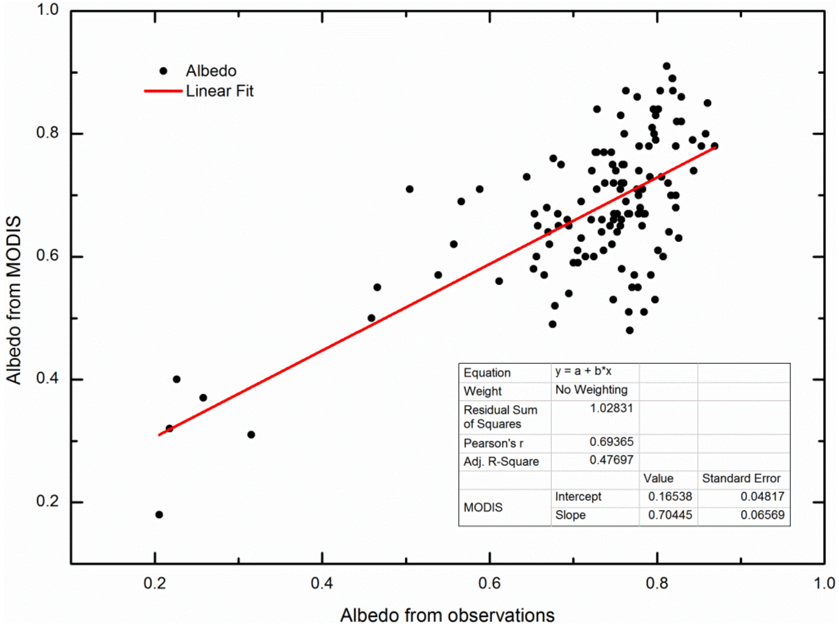

Equation	y = a + b*x		
Weight	No Weighting		
Residual Sum of Squares	1.02831		
Pearson's r	0.69365		
Adj. R-Square	0.47697		
		Value	Standard Error
MODIS	Intercept	0.16538	0.04817
	Slope	0.70445	0.06569

Figure 3. The albedo of the pixel including AWS in Zhadang glacier derived from MODIS and that observed by AWS in 2011.

Title Page
Abstract Introduction
Conclusions References
Tables Figures
I◀ ▶I
◀ ▶
Back Close
Full Screen / Esc
Printer-friendly Version
Interactive Discussion

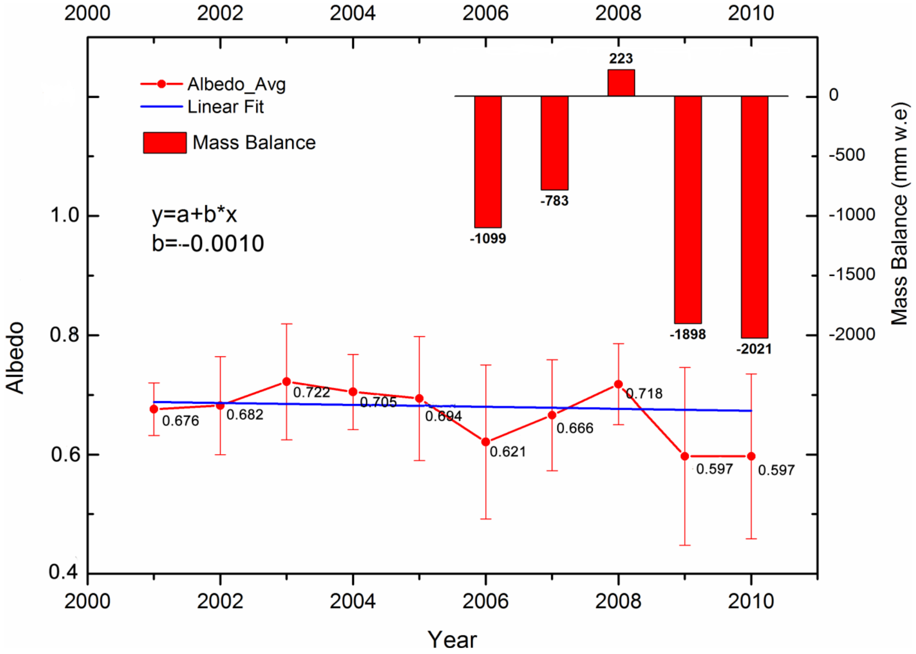

Figure 4. Temporal changes of albedo in Zhadang glacier during 2000 to 2010 and mass balance from 2006 to 2010. The albedo of Zhadang glacier showed a downward trend in the past 10 years overall. There is a significant positive correlation between albedo and the negative mass balance ($R^2 > 0.95$, passed the statistical significance test at 0.01 level).

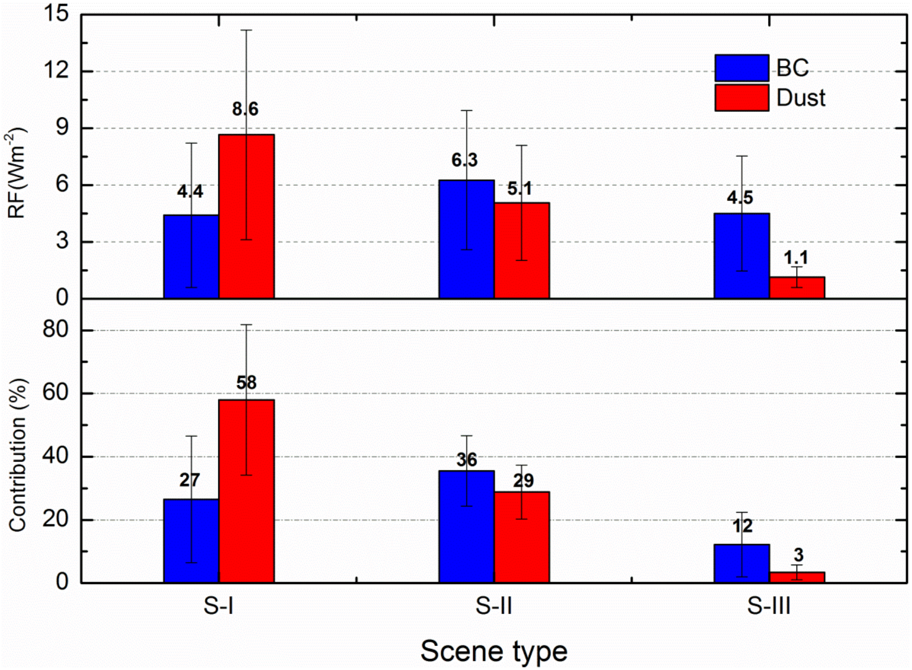

Figure 5. RF of BC and dust on the Zhadang glacier and the contribution (results from SNICAR model) show the reduction of albedo in the surface snow cover area under three different melting conditions: S-I, where the surface of the glacier is bare ice; S-II, where the glacier is covered by aged snow; S-III, where the glacier is covered by fresh snow.

Title Page
Abstract
Introduction
Conclusions
References
Tables
Figures
I◄
►I
◄
►
Back
Close
Full Screen / Esc
Printer-friendly Version
Interactive Discussion